POZNAN UNIVERSITY OF TECHNOLOGY ACADEMIC JOURNALS
No 93 Electrical Engineering 2018

DOI 10.21008/j.1897-0737.2018.93.0017

Michał BEREŹNICKI*, Paweł JABŁOŃSKI*

CALCULATIONS OF MACROSCOPIC EDDY CURRENT LOSSES IN FERROMAGNETIC MATERIALS CONSIDERING HYSTERESIS LOOP

The paper presents an algorithm for calculation of eddy current power losses caused by macroscopic eddy currents in ferromagnetic materials considering non-linearity of magnetization characteristics and magnetic hysteresis. The results of calculations are presented for a typical non-oriented steel sheet with silicon content of 6.5%. It has been found that inclusion of hysteresis loop and non-linearity of magnetization for the analyzed material has little effect on the calculated eddy current losses. Restrictions on the use of the algorithm are primarily due to the assumption of average values of the flux in the cross section of the sample, numerical problems when converting B → H and H → B for large increases in the induction, and the lack of regularity of the shape of the hysteresis loop measurements.

KEYWORDS: eddy current power losses, magnetic hysteresis, magnetic nonlinearity.

1. INTRODUCTION

Magnetic materials are widely used in the construction of electrical machines. Lossiness is one of the basic parameters of magnetic materials and is described by empirical and theoretical formulas [1-5]. According to the classical approach, losses in magnetic materials are associated with eddy currents and magnetization change (hysteresis losses). Eddy current losses are often represented as the sum of macroscopic eddy current losses and the so-called excess losses, yet this approach is sometimes criticized. Macroscopic eddy current losses are usually determined with vastly simplifying assumptions, including both sinusoidal induction and strength of magnetic field in the sample. However, due to non-linearity and hysteresis, these waveforms cannot be sinusoidal at the same time. It is therefore advisable to examine how consideration of non-linearity and hysteresis loop affects classical (i.e. macroscopic) eddy current losses. One of the attempts to take non-linearities into account is described in [7]. The paper presents an algorithm for calculating eddy current losses for sheets with known characteristics of magnetization, and with the assumption that

* Czestochowa University of Technology

the flux is sinusoidal. Considering hysteresis in this type of losses seems to be the next step and is also the goal of this work. The paper employs appropriately modified algorithm described in [7].

2. CLASSICAL MACROSCOPIC EDDY CURRENT LOSSES

Theoretical description of macroscopic eddy current losses in a conductive cuboidal magnetic sample is presented in several works, e.g. [3, 8]. Starting from Maxwell's equations, using the Poynting theorem and making a number of additional simplifications (e.g., it was assumed that the vector of magnetic field has only one spatial component, and the fields change over time sinusoidally at each point of the sample) the following relationship for the classical eddy current loss per unit of volume of the sample is achieved:

$$P_{\mathrm{cl}} = \frac{\pi f B_{\mathrm{m}}^2 \gamma}{2\mu}\left(\frac{\sinh\gamma - \sin\gamma}{\cosh\gamma - \cos\gamma}\right) \tag{1}$$

where: f – frequency, B_{m} – maximum flux density, μ – magnetic permeability, and

$$\gamma = \frac{g}{\delta} \tag{2}$$

where: g – thickness of the sample, δ – replacement field penetration depth defined by the formula:

$$\delta = \frac{1}{\sqrt{\pi\sigma\mu f}} \tag{3}$$

where: σ – conductivity of the material.

Formula (1) takes into account the skin effect, but does not include any nonlinearity and hysteresis. This issue was analyzed among others in [6]. Below we constructed an algorithm which takes into account known hysteresis loops.

3. EDDY CURRENT POWER LOSSES WITH HYSTERESIS TAKEN INTO ACCOUNT

3.1. Governing equations

To reflect the impact of the phenomenon of magnetic hysteresis on macroscopic eddy current loss, a cuboidal sample with thickness g, height $a \gg g$ and length $l \gg g$ was considered. The middle of the sheet was adopted as the origin of the coordinate system (Fig.1). The governing field equations in this case are as follows:

$$\nabla \times \mathbf{H} = \mathbf{J} \tag{4}$$

$$\nabla \times \mathbf{E} = -\frac{\partial \mathbf{B}}{\partial t} \tag{5}$$

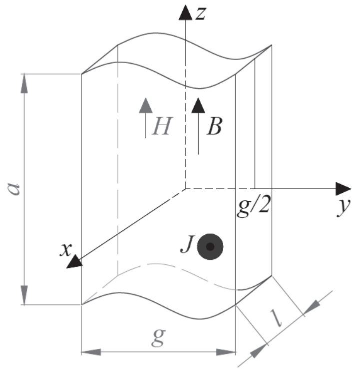

Fig. 1. The geometry of the analyzed sample

where ***H*** – vector of magnetic field intensity, ***J*** – vector of current density, ***E*** – vector of electric field intensity, ***B*** – vector of magnetic flux density. Throughout the volume of the sample the point form of Ohm's law is fulfilled:

$$\mathbf{J} = \sigma \mathbf{E} \tag{6}$$

Between the vectors ***B*** and ***H*** there is a relationship resulting from the process of magnetization of the sample, which can be presented in the general form as:

$$\mathbf{B} = f_{\mathrm{HB}}(\mathbf{H}) \tag{7}$$

where f_{HB} specifies the ***H-B*** characteristics, and in the analyzed case will correspond with the hysteresis loop. Below it is assumed that ***B*** has only a component in the *z* direction, and depends only on the coordinate *y* and time:

$$\mathbf{B} = B_z(y,t)\hat{\mathbf{z}} \tag{8}$$

Disregarding the possible anisotropy of the sample, a vector ***H*** is obtained, also only with the component *z,* dependent on *y*:

$$\mathbf{H} = H_z(y,t)\hat{\mathbf{z}} \tag{9}$$

Then, Eq. (4) gives:

$$\mathbf{J} = \frac{\partial H_z(y,t)}{\partial y}\hat{\mathbf{x}} = J_x(y,t)\hat{\mathbf{x}} \tag{10}$$

Next, Eq. (5) when multiplied by σ fields:

$$-\sigma \frac{\partial B_z(y,t)}{\partial t}\hat{\mathbf{z}} = -\frac{\partial(\sigma E_x(y,t))}{\partial y}\hat{\mathbf{z}} = -\frac{\partial J_x(y,t)}{\partial y}\hat{\mathbf{z}} \tag{11}$$

Hence, we finally get the following set of equations to be solved:

$$\frac{\partial J_x(y,t)}{\partial y} = \sigma \frac{\partial B_z(y,t)}{\partial t} \tag{12}$$

$$\frac{\partial H_z(y,t)}{\partial y} = J_x(y,t) \tag{13}$$

$$B_z = f_{\mathrm{HB}}(H_z), \quad H_z = f_{\mathrm{BH}}(B_z) \tag{14}$$

where: f_{HB} and f_{BH} are mutually inverse relationships between B_z and H_z. They can be vertex characteristics or hysteresis loop family. These equations are solved iteratively, assuming that the total magnetic flux through the sample, $\Phi(t)$, varies sinusoidally in time, or considering the average induction as follows:

$$B_{\mathrm{av}}(t) = \frac{\Phi(t)}{gl} = B_{\mathrm{m}} \sin \omega t \tag{15}$$

After determining the vector of density of eddy currents $\boldsymbol{J}$, the macroscopic eddy current losses are calculated as periodical average from losses caused by the flow of eddy currents in a volume unit of the sample:

$$P_{\mathrm{eddy}} = \frac{1}{T}\int_0^T \left(\frac{1}{gbl} \iiint_\Omega \frac{\mathbf{J}\cdot\mathbf{J}}{\sigma} \mathrm{d}\Omega \right) \mathrm{d}t = \frac{4f}{\sigma g} \int_{t=0}^{\frac{1}{2f}} \int_{y=0}^{\frac{1}{2}g} J_x^2\left(y,t\right) \mathrm{d}y\, \mathrm{d}t \tag{16}$$

3.2. Algorithm for solving the field equations

The algorithm for solving the field equations is show in Fig. 2. In the first step, we assume a certain time-space distribution of magnetic flux density retaining the sinusoidal flux according to Eq. (15). Based on the flux density distribution, we determine the density of eddy currents, and then the distribution the magnetic field intensity. From the measured hysteresis loop family, we read the B-field corresponding to the calculated H-field. Then the B-field is corrected so that the magnetic flux remains sinusoidal. If the difference between the obtained induction of the current step and the previous step is not greater than the assumed value ε, as below:

$$\max \left| \Delta B^{(k)}(y,t) \right| \le \varepsilon B_{\mathrm{m}} \tag{17}$$

then we finish the iterative process, otherwise we repeat the calculation sequence. Another condition for finishing the calculations is reaching the maximal permitted number of iterations.

Assuming the presented algorithm converges, the density of the induced eddy currents is obtained $J_x(y, t)$, which in turn allows the macroscopic eddy current losses to be calculated via Eq. (16).

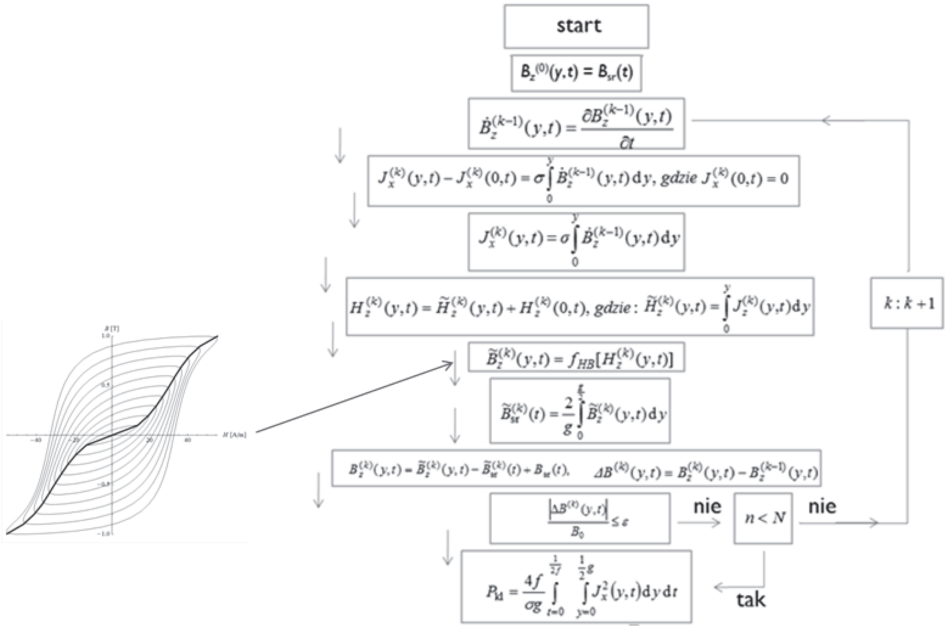

Fig. 2. Block diagram of the algorithm

3.3. Implementation aspects

The implementation of the algorithm involves a number of steps, such as: numerical differentiation, numerical integration, and above all – conversion between ***H*** and ***B*** via a given family of hysteresis loops. These issues are extremely important from the numerical point of view.

If a vertex curve *B-H* is defined in the form of points (H_i, B_i), the conversion $H \to B$ and $B \to H$ using piecewise is relatively simple (Fig. 3). When using the hysteresis loop, the relationship $B(H)$ is a family of hysteresis loops corresponding to different values $B_{\max}$ or $H_{\max}$. The conversion $B \to H$ and vice versa involves two problems: which of the loops to choose – Fig. 4a, and which of the two values of *H* corresponding to one value *B* to select (Fig. 4b).

Solution to the first question requires knowledge of not only the induction *B* itself, but also the maximum induction $B_{\max}$. We continue to assume that we have a family of hysteresis loops taken by the sinusoidal variation $B(t)$. Knowledge of magnetic flux density amplitude ($B_{\max}$) allows us to identify the loop which corresponds to the sinusoid $B(t)$. Typically, this loop is in between the measured loops, and can therefore be determined by linear interpolation from the two adjacent loops.

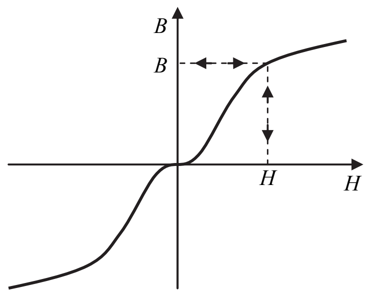

Fig. 3. Conversion $H \rightarrow B$ and $B \rightarrow H$ by vertex curve

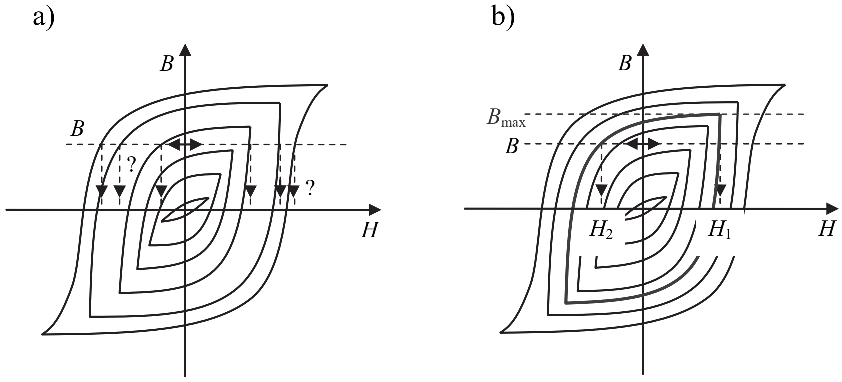

Fig. 4. Ambiguity of transformation $B \rightarrow H$:
a) which loop to choose b) which value of H to choose?

If $B \neq \pm B_{max}$, another question arises, i.e. which of the two H-field values to choose? For this purpose, the sign of derivative of B is inspected. If B is increasing, right branch is selected and the value of H_1 obtained. If B is decreasing, left branch is selected, which gives H_2.

A similar procedure is performed during the conversion $H \rightarrow B$. In the general case, the loop is broken into left and right branches during conversion $B \rightarrow H$ and into the upper and lower branches during conversion $H \rightarrow B$ (Fig. 5).

It should be emphasized that the discussed procedure for considering hysteresis loop is affected by a number of imperfections:

– the hysteresis loops are determined by measurements of the average value of the sinusoidally varying induction, while at various points y the waveforms $B_z(y, t)$ are not necessarily sinusoidal,
– hysteresis loops taken during measurements refer to the sample as a whole, while the loops are used to convert local field values,

- there are problems with the convergence of the algorithm when the loops have shapes that deviate from the assumed "regular", i.e. when there are more than two values of *B* corresponding to *H* or vice versa,
- if the loop contains sections with very steep slope ($dB/dH \to \infty$), the error of conversion $H \to B$ is significant (small change in *H* strongly changes *B*), and influences the convergence of the algorithm.

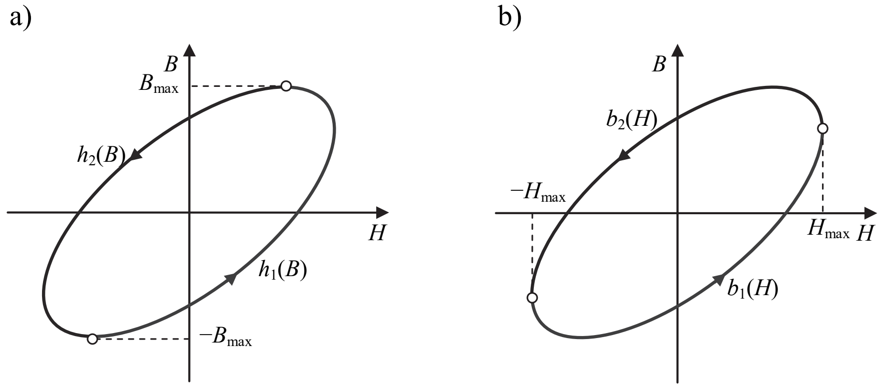

Fig. 5. Breakdown of the hysteresis loop:
a) into left and right branches, b) into upper and lower branches

4. CALCULATION RESULTS

The presented algorithm was used to determine macroscopic eddy current losses in non-oriented 6.5% Si-Fe steel in the form of a sheet of dimensions 500 mm × 500 mm, with thickness $g = 0.1$ mm and conductivity $\sigma = 1.22 \times 10^6$ S/m, for frequencies in the range 10-400 Hz, and induction B_m within 0,1-1,2 T. The measurements were made in accordance with applicable standards IEC 60404-2, 60404-6, using the computerized measuring system MAG-RJJ-2.0. Hysteresis loop family for 400 Hz is shown in Fig. 6.

The calculations were made in two versions – without taking into account the hysteresis loop (with magnetization curve in the form of a vertex curve), and taking into account the hysteresis loop family. It was assumed that the condition for the completion of iteration is achieving the relative permissible error not greater than $\varepsilon = 0.001$ or performing up to 20 iterations. In some cases we failed to reach the assumed accuracy, however, the maximum relative error was less than 0.04, which can be considered acceptable. It should be noted that increasing the number of iterations did not result in reduction of the error. The reason for the lack of convergence of the algorithm may be the method of *B-H* conversion and restrictions described in the previous chapter.

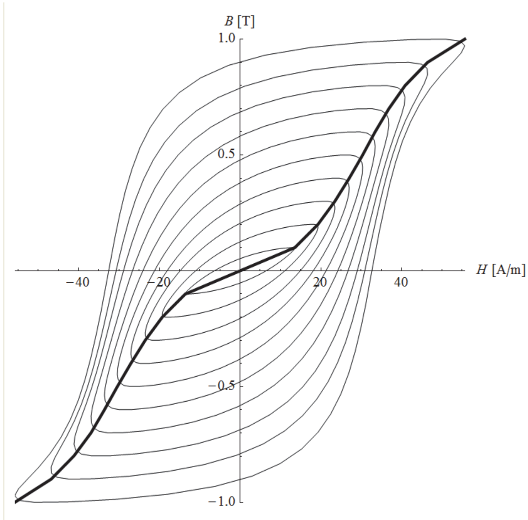

Fig. 6. Hysteresis loop family obtained from measurements for f = 400 Hz, BNO 6.5% Si; also vertex magnetization curve is depicted

The resulting loss of power – formula (16) – was compared with calculated values according to Eq. (1) by calculating the relative error:

$$\delta_P = \frac{P_{\mathrm{eddy}} - P_{\mathrm{cl}}}{P_{\mathrm{cl}}} \times 100\% \tag{18}$$

For the value of magnetic permeability μ occurring in Eq. (1) we assumed:

$$\mu = \frac{B_{\mathrm{m}}}{f_{\mathrm{HB}}(B_{\mathrm{m}})} \tag{19}$$

Calculation results are presented in figures 7-8. They represent the dependence of δ_P on B_{m} for the selected frequency and the relationship of δ_P on frequency f for the selected values B_{m}. The calculation results indicate that taking into account the hysteresis loop in macroscopic eddy current losses has a relatively small effect, at least for the tested magnetic materials magnetized in the considered conditions. The relative error of the calculated power loss related to the losses calculated according to the general formula did not exceed: 0.2% for the calculations which take into account the non-linearity defined with the vertex curve and 2.4% for the calculation taking into account the hysteresis loop. It should be noted, however, that the tested sample had a rather small thickness of 0.1 mm – for higher thicknesses the difference δ_P may be greater.

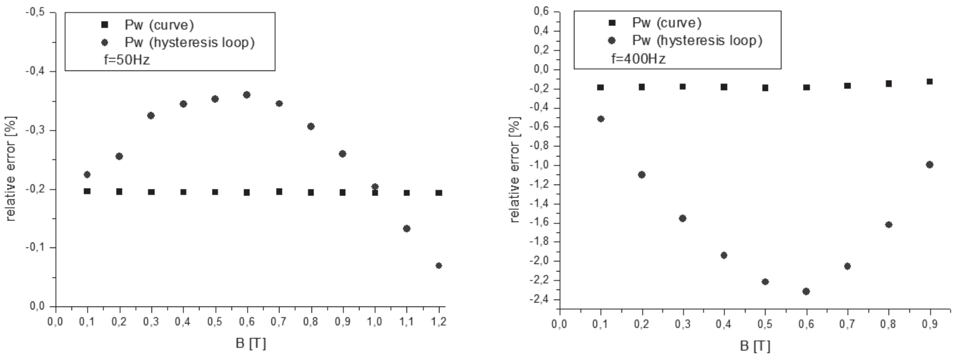

Fig. 7. Relative error for eddy current power loss calculated according to the algorithm related to the classic loss, f = 50 Hz and f = 400 Hz, BNO 6.5% Si (black squares – calculations with vertex curve, red dots – calculations with hysteresis loop family)

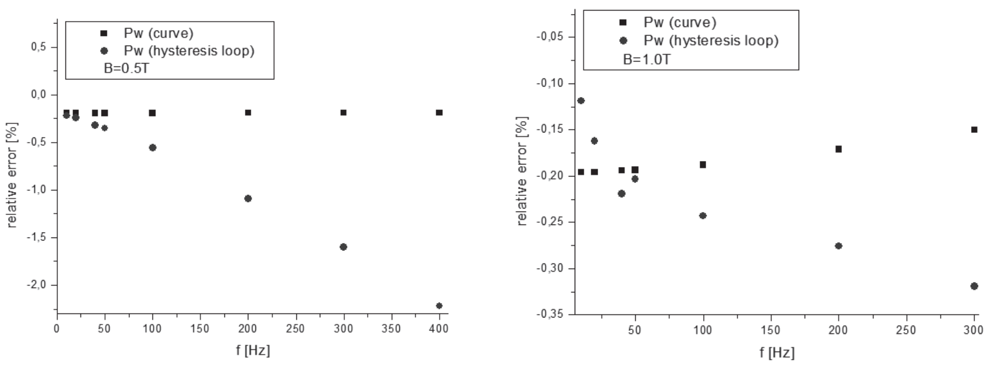

Fig. 8. Relative error for eddy current power loss calculated according to the algorithm related to the classic loss, B = 0,5 T and B = 1.0 T, BNO 6.5% Si (black squares – calculations with vertex curve, red dots – calculations with hysteresis loop family)

5. CONCLUSIONS

The paper presents the algorithm for calculating the macroscopic eddy current power losses in ferromagnetic materials taking into account the non-linearity of the magnetization characteristics and the phenomenon of magnetic hysteresis. With its help, calculations of classical eddy current power losses were made for a 6.5% Si-Fe non-oriented electrical steel sheet. The results indicate that taking into account the hysteresis loop or the non-linearity alone for the tested material has a relatively small effect on the value of macroscopic eddy current power losses. The relative difference between the losses calculated according to the algorithm, and losses calculated according to the classic formula did not exceed 0.2% for the calculations which take into account the non-linearity defined by the vertex curve, and 2.4% for the calculation taking into account the hysteresis loop.

The presented algorithm is not without limitations, especially the conversion $B \rightarrow H$ and $H \rightarrow B$ according to the defined family of hysteresis loops needs to be improved. This will be the subject of further consideration.

REFERENCES

[1] Krings A., Soulard J., Overview and comparison of iron loss models for electrical machines, in Proceedings of International Conference on Ecological Vehicles and Renewable Energies EVER 2010, March 25-28 2010, Monaco, abridged version published in Journal of Electrical Engineering (ISSN 1582-4594) Vol. 10/2010 No. 3, paper 10.3.22.
[2] C. Steinmetz: On the law of hysteresis (oryginał opublikowany in 1892), Proceeding of the IEE, vol. 72/2010 no. 2, pp. 197-221, 1984.
[3] Barranger J., Hysteresis and eddy-current losses of transformer lamination viewied as an apllication of the Pointing Theorem, NASA Technical Note, D-3114, 1965.
[4] Bertotti G., Some considerations on the physical interpretation of eddy current losses in ferromagnetic materials, J. Magn. Mater. 1986, vol. 54-57, pp. 1556-1560.
[5] Zirka S.E., Moroz Y.I., Marketos P., Moses A.J., Loss separation in nonoriented electrical steels, IEE Trans. Magn. 2010, vol. 46, pp. 286-289.
[6] Bereźnicki M., The influence of skin effect on the accuracy of eddy current energy loss calculation in electrical steel sheets, IEEE, Selected Problems of Electrical Engineering and Electronics (WZEE), 2015, 17-19 Sept. 2015.
[7] Górecki J., Nowak L., Poltz J., Numerical calculation of eddy current losses in conductive ferromagnetic plate, Electrical hearings in 1976, 22, z. 3, pp. 677-685
[8] G. Bertotti, Hysteresis in magnetism, Academic Press, San Diego (1998).

(Received: 08.02.2018, revised: 09.03.2018)